Stimulated Photon Echoes from Amide I Vibrations

Peter Hamm,[†] Manho Lim,[‡] William F. DeGrado, and Robin M. Hochstrasser*

Department of Chemistry and Department of Biophysics and Biochemistry, Johnson Foundation, University of Pennsylvania, Philadelphia, Pennsylvania 19104-6323, and Max Born Institut, 12489 Berlin, Germany

Received: June 2, 1999

The amide I band region (ca. 1650 cm^{-1}) of two small globular peptides, apamin and a *de novo* cyclic pentapeptide, has been investigated by stimulated (three pulse) photon echo experiments. In both samples, a large shift (250 fs) of the first moment of the echo signal was found, which decays on a 3−5 ps time scale. A simple Bloch formalism is used to calculate the four-wave mixing signal from the excitonically coupled amide I states. The mechanisms responsible for the deviation of the first moment from zero are discussed with the help of model simulations. The decay of the first moment, which is not predicted by the Bloch description, is due to spectral diffusion processes caused by equilibrium fluctuations of the peptide backbone and amide oscillators.

1. Introduction

The three-dimensional structure of peptides and proteins are essential for the selectivity and specificity of biological reactions. While very powerful experimental tools such as X-ray scattering and NMR spectroscopy exist for protein structure determination, the dynamics of these structures are more elusive and often require computer simulations. Experimental feedback that can verify such molecular dynamic (MD) simulations is scarce. It is well accepted that it is not only the three-dimensional structure of proteins that is essential for the functionality of proteins but also the equilibrium fluctuations around the time-averaged structure.[1,2] One prominent example is the observation that oxygen would never reach the binding site in myoglobin if the structure obtained from X-ray data were static. MD simulations, however, show that fluctuations of the peptide backbone and side chains over a wide frequency range open transient paths to the binding side.[1,3] One may assume that the evolution process of nature has optimized not only the structures of biomolecules but also their dynamics.

One approach to obtain important information on the dynamics and structure of proteins is by means of coherent nonlinear infrared spectroscopy.[4−6] For example, a form of two-dimensional or correlation infrared spectroscopy that was recently introduced[4,5] has the potential to enable the determination of peptide structures on essentially any desired time scale. Typically in such an experiment a set of coupled vibrational states representing the peptide undergoes a nonlinear interaction with a controlled sequence of femtosecond infrared pulses. The couplings between the vibrational excitations, which are highly dependent on the three-dimensional structure of the peptide, are evidenced by the off-diagonal peaks of these two-dimensional spectra. The strengths of the off-diagonal peaks depend on the distance and relative orientation of the pairs of local vibrations. The development of a structure consistent with the 2D spectra would be based on a theoretical description of the vibrational modes and their coupling, as well as on knowledge of the relaxation parameters associated with the vibrational states. Approaches based on these principles could then be used to examine the evolution of peptide conformational changes and chemical reactions with subpicosecond time resolution.

The interpretation of our previous investigations[4,5] incorporated a model introduced by Krimm et al.[7] and further specified by Tasumi et al.,[8] according to which the amide I band of proteins can be viewed as an excitonically coupled system, with the dominant coupling mechanism being the transition dipole interaction. Experiments on the amide I vibrational mode of the peptide backbone enabled a determination of the strength of coupling between pairs of peptide groups with the help of cross peaks,[4,5] in analogy to two-dimensional NMR spectroscopy (COSY).[9] With the help of these 2D-IR experiments, the excitonic coupling model has been verified for the first time with natural peptides, and parameters for dephasing, disorder, and degree of delocalization have been established. A second approach involves femtosecond stimulated (three-pulse) photon echoes of vibrational transitions of small molecular probes bound to enzymes such as carbonic anhydrase and hemoglobin.[6] The echo experiments prove that the vibrational frequency fluctuation correlation function decays on many time scales ranging from 100 fs to beyond tens of picoseconds. These experiments are conceptually similar to electronic photon echoes of immobilized chromophores.[10−13] However, the IR signals are highly sensitive to the local fluctuations of the enzyme binding pocket, since the short-range anharmonic interaction between the test molecule and the surroundings is responsible for the spectral diffusion of vibrational frequencies.

While the first type of experiment has been interpreted in terms of the static structure of the peptide, the second, which is sensitive to the dynamics of the enzyme pocket, measures the influence of the fluctuating surroundings (i.e., the peptide) on the vibrational frequency of a test molecule, rather than the fluctuations of the peptide backbone itself. What we present in this paper is a first attempt to combine both concepts and measure the stimulated photon echo of the amide I band directly. The two peptides selected for these experiments have been studied in previous work:[4,5] apamin,[14] a small neurotoxic peptide

* Corresponding author. E-mail: hochstra@sas.upenn.edu. Fax: 215-898-0590.

[†] Max Born Institut.

[‡] Present address: Department of Chemistry, College of Natural Science, Pusan National University, Republic of Korea.

10.1021/jp9917650 CCC: $18.00
Published on Web 08/21/1999

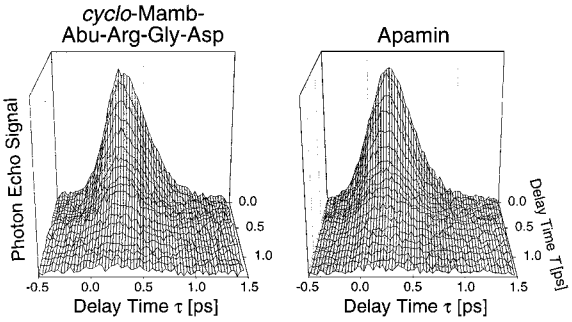

Figure 1. Stimulated (three pulse) photon echo signal of the cyclic pentapeptide (*cyclo*-Mamb-Abu-Arg-Gly-Asp)[15] and apamin as a function of delay time τ, which denotes the separation between the peaks of the first and second pulse, and T, which denotes the separation between the second and the third pulse.

found in the bee venom, which consists of 18 amino acids forming a short piece of an α-helix and a β-turn, and a *de novo* cyclic model system (*cyclo*-Mamb-Abu-Arg-Gly-Asp).[15] Because there are only five amide I transitions underneath the amide I band in the cyclic pentapeptide, and these are spectrally resolved in the IR absorption spectrum, it was possible to estimate all the elements of the coupling Hamiltonian for this case.[5]

2. Material and Methods

Tunable IR pulses having pulse duration 120 fs, energy ca. 1 μJ, bandwidth ca. 150 cm^{-1}, and frequency tuned to the center of the amide I band (ca. 1650 cm^{-1}) were generated by mixing the signal and the idler output of a BBO-optical parametric amplifier in a $AgGaS_2$ crystal.[16] The output was split into three beams (labeled k_1, k_2, and k_3) with parallel polarization and approximately the same energy (300 nJ). The pulses with wave vectors k_1 and k_3 traversed computer-controlled delay lines. The three beams were focused at the sample (spot size 150 μm) in a box configuration.[17] An MCT detector recorded the signal in the $-k_1 + k_2 + k_3$ phase matching direction. Delay zero between all pulses was obtained with an accuracy of ca. $\pm$50 fs by measuring induced multiphoton absorption of the k_2 beam in a thin germanium sample.

Apamin was purchased from Sigma, prepared as described in ref 4, and dissolved in D_2O at a concentration of 15 mM (pH 4). The cyclic model peptide, *cyclo*-Mamb-Abu-Arg-Gly-Asp,[15] was dissolved in D_2O at a concentration of ca. 50 mM and buffered at pH 3.5. The samples were held in a CaF_2 cell with a spacing of 25 μm.

3. Experimental Results

Figure 1 shows the stimulated photon echo signal of the cyclic pentapeptide (*cyclo*-Mamb-Abu-Arg-Gly-Asp)[15] and apamin. The photon echo signal is recorded as a function of two time intervals τ and T, where τ (which can be negative or positive) denotes the separation between the peaks of pulse k_1 and k_2, while T, the separation between the second and the third light interaction, is defined as the separation between the peaks of pulse k_2 and pulse k_3 for $\tau > 0$, or between the peaks of pulse k_1 and pulse k_3 for $\tau < 0$, respectively. Qualitatively, the responses of both samples are similar. The signal is peaked at ca. $\tau = +250$ fs in both cases, it is not symmetric with respect to the peak position, and it decays more rapidly toward smaller delay times τ. The asymmetry is somewhat more pronounced in the case of the cyclic pentapeptide. In the direction of the T-axis, an overall decay of the signal is found. A single-exponential fit of the transient grating signal (i.e., the signal along the T-axis for $\tau = 0$, black squares in Figure 2) yields a time constant of ca. 400 fs in both cases. A somewhat better fit is obtained with two exponentials having time constants of 250 and 600 fs (see Figure 2)

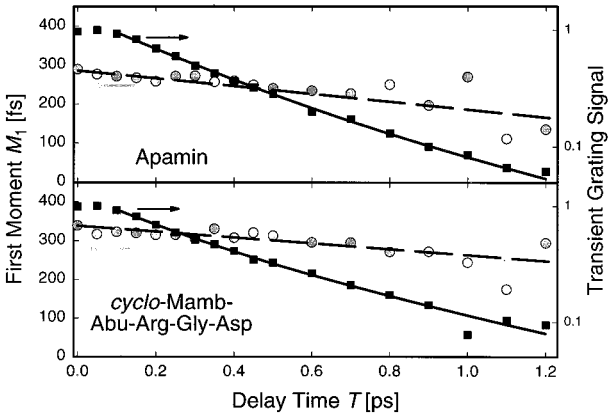

Figure 2. Normalized first moment (gray circles, left scale) and transient grating signal (black squares, right scale) of the data shown in Figure 1.

In stimulated photon echo experiments on isolated vibrational transitions,[6,18] the normalized first moment (as a function of T)

$$M_1(T) = \int_{-\infty}^{\infty} \tau \cdot S(T,\tau)\, d\tau / \int_{-\infty}^{\infty} S(T,\tau)\, d\tau \qquad (3.1)$$

is a convenient measure of the asymmetry of the signal with respect to $\tau = 0$. The first moment, which is shown in Figure 2 (gray circles) is slightly larger in the case of the cyclic pentapeptide as compared with apamin. Both signals decay slightly within the observation window of 1.2 ps, and a time constant of 3$-$5 ps can be estimated by extrapolation of the data assuming the observed decay is the early part of a single exponential. This procedure generates a lower limit for the time scale of the decay of the first moment signal. It should be mentioned that stimulated photon echo work on electronic two-level systems was usually displayed by means of the shift of the echo peak from zero on the τ axis.[19$-$21] The experimental first moment data and the peak shift[11,22] data are both qualitative representations of the time evolution of the transition frequency fluctuations. The actual correlation function, which can be deduced from the complete data set, gives the relaxation times of the inhomogeneous distribution.

4. Theoretical Modeling

The inhomogeneity and spectral diffusion of electronic[19$-$21] and vibrational[6,18] transitions were examined using three-pulse photon experiments in which the signals under rephasing ($\tau > 0$) and nonrephasing ($\tau < 0$) conditions are compared. However, the interpretation of such experiments becomes considerably more complex when instead of a single isolated anharmonic oscillator undergoing spectral diffusion,[6,18] there is a set of excitonically coupled transitions.[4,5] In the following a simple model is developed for a system of coupled oscillators assuming a strict separation of time scales that implies a homogeneous dephasing in a fixed inhomogeneous distribution of transitions. The application of the data to a theory that includes both vibrational energy transfer and spectral diffusion processes[23,24] is left for future work.

In a third-order experiment, such as the stimulated photon echo described here, it is necessary to consider transitions from the ground state $\{|0\rangle\}$ to the n one-excitonic states $\{|i\rangle\}$, and

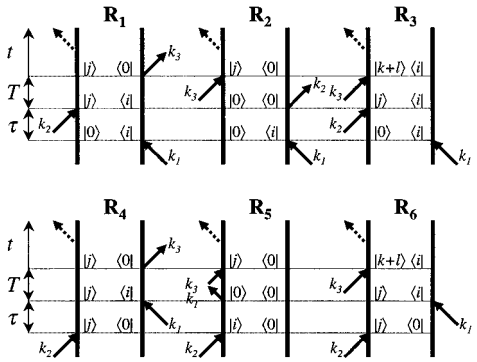

Figure 3. Feynman diagrams, which have to be taken into account to model the experimental data. R_1, R_2, R_3 are the Feynman diagrams relevant for rephasing conditions (photon echo), while R_4, R_5, R_6 describe the nonrephasing four-wave mixing signal (reverse photon echo).

from these to the $1/2n(n+1)$ two excitonic states $\{|i+j\rangle\}$, where n is the number of peptide groups in the protein. Although the labeling, $|i+j\rangle$, used here for the two-excitonic states is just a way of numbering them and therefore is fully general, it emphasizes that the two-excitonic states are, in the harmonic limit, products of the (harmonic) one-excitonic states. This parentage is especially appropriate in the perturbation limit where the anharmonicity or coupling is small compared with the diagonal energy differences. The eigenvalues and the transition dipoles between all the states are determined by diagonalization of the coupling Hamiltonian, which is related to the three-dimensional structure of the peptide.[4,5]

All the possible transitions involving these one and two exciton states are expected to lie within the range of the ca. 150 cm^{-1} spanned by the bandwidth of the laser pulses and thus have to be included in the treatment. The relevant Feynman diagrams are shown in Figure 3. Assuming Bloch dynamics the response functions corresponding to each of the diagrams can be obtained by inspection:

$$R_1 = \sum_{i,j}\langle \mu_{0,i}^2\,\mu_{0,j}^2\rangle e^{i(\epsilon_i\tau-\epsilon_j t)}\, e^{i(\epsilon_i-\epsilon_j)T}\, e^{-(\tau+t)/T_2}\, e^{-T/T_1} \quad (4.1)$$

$$R_2 = \sum_{i,j}\langle \mu_{0,i}^2\,\mu_{0,j}^2\rangle e^{i(\epsilon_i\tau-\epsilon_j t)}\; e^{-(\tau+t)/T_2}\, e^{-T/T_1} \quad (4.2)$$

$$R_3 = \sum_{i,j,k\le l}\langle \mu_{0,i}\,\mu_{0,j}\,\mu_{j,l+k}\,\mu_{l+k,i}\rangle e^{i(\epsilon_i\tau-(\epsilon_{kl}-\epsilon_i)t)} \times e^{i(\epsilon_i-\epsilon_j)T}\, e^{-(\tau+t)/T_2}\, e^{-T/T_1} \quad (4.3)$$

$$R_4 = \sum_{i,j}\langle \mu_{0,i}^2\,\mu_{0,j}^2\rangle e^{i\epsilon_j(\tau+t)}\, e^{i(\epsilon_i-\epsilon_j)T}\, e^{-(\tau+t)/T_2}\, e^{-T/T_1} \quad (4.4)$$

$$R_5 = \sum_{i,j}\langle \mu_{0,i}^2\,\mu_{0,j}^2\rangle e^{i(\epsilon_i\tau+\epsilon_j t)}\; e^{-(\tau+t)/T_2}\, e^{-T/T_1} \quad (4.5)$$

$$R_6 = -\sum_{i,j,k\le l}\langle \mu_{0,i}\,\mu_{0,j}\,\mu_{j,l+k}\,\mu_{l+k,i}\rangle e^{-i(\epsilon_j\tau+(\epsilon_{kl}-\epsilon_i)t)} \times e^{i(\epsilon_i-\epsilon_j)T}\, e^{-(\tau+t)/T_2}\, e^{-T/T_1} \quad (4.6)$$

where the time intervals τ, T, and t, are defined in Figure 3. The $\mu_{0,i}$ and the $\mu_{i,l+k}$ are the projections onto the incident field polarization axis of transition dipoles between the ground state and the one-excitonic states and between the one and the two-excitonic states, respectively. All the pulses are polarized in the same laboratory-fixed direction. The homogeneous dephasing rate $1/T_2$ is assumed to be the same for transitions between ground and one-excitonic states, as between one-excitonic and two-excitonic states. This assumption is supported by studies of model compounds where the spectral line widths of the $0 \rightarrow 1$ and $1 \rightarrow 2$ amide transitions are approximately equal.[4] Population relaxation from the one-excitonic states into the ground state is designated by T_1. Again, studies of model compounds, peptides, and proteins have shown that the amide T_1 relaxation is always ca. 1 ps and therefore a property of the amide unit.[4] It is therefore expected to be a property shared by each exciton state. Population equilibration and dephasing within the one-excitonic manifold is neglected at this stage (see discussion). The bracket $\langle\cdots\rangle$ denotes an orientational average where the corresponding direction cosines are:

$$\langle \mu_{0,i}\,\mu_{0,j}\,\mu_{j,l+k}\,\mu_{l+k,i}\rangle \equiv \langle \mu_a\mu_b\mu_c\mu_d\rangle = {}^1/_{15}|\mu_a\mu_b\mu_c\mu_d|(\cos\varphi_{ab}\cos\varphi_{cd} + \cos\varphi_{ac}\cos\varphi_{bd} + \cos\varphi_{ad}\cos\varphi_{bc}) \quad (4.7)$$

with the φ's are the angles between the indicated transition dipoles and the prefactor is the product of their magnitudes.

Equations 4.1−4.3 can be simplified significantly in the weak coupling limit,[5] where each excitation is predominantly localized on one individual peptide site, and the states are perturbed only by diagonal, $\epsilon_{ii} = 2\epsilon_l - \Delta\epsilon_{ii}$, and off-diagonal (intermode) anharmonicity $\epsilon_{ij} = \epsilon_l + \epsilon_j - \Delta\epsilon_{ij}$.[5] Then, transitions such as $|i\rangle \rightarrow |l+k\rangle$, $i \neq k,l$, can be neglected ($\mu_{i,l+k} = 0$) and the transition dipole moments of the allowed transitions are $\mu_{i,i+j} = \mu_{0,j}$, $i \neq j$, and $\sqrt{2}\mu_{0,i}$. The total response function then reduces to

$$\sum_{l=1}^{3} R_l = \sum_{i,j}\langle \mu_{0,i}^2\,\mu_{0,j}^2\rangle e^{i(\epsilon_i\tau-\epsilon_j t)}[1 + e^{i(\epsilon_i-\epsilon_j)T}] \times [1 - e^{i\Delta\epsilon_{ij}t}]e^{-(\tau+t)/T_2}\, e^{-T/T_1} \quad (4.8)$$

which is exactly zero in the harmonic limit ($\Delta\epsilon_{ij} = 0$), as expected.

The detector measures the t-integrated intensity of the third-order polarization:

$$S(\tau,T) = \int_0^\infty |P^{(3)}(\tau,T,t)|\, dt \quad (4.9)$$

where the third-order polarization is obtained by convoluting the response functions $\sum_{l=1}^{3} R_l$ (or $\sum_{l=4}^{6} R_l$, depending on the time ordering) with the electric fields[25] and averaging over any inhomogeneous distribution.

In a previous paper,[5] the 2D-IR spectrum of the cyclic pentapeptide was investigated in detail and the underlying one-exciton Hamiltonian was deduced from the intensities of the off-diagonal peaks. Parameters for homogeneous broadening ($T_2 = 0.9$ ps) and diagonal disorder (inhomogeneous broadening, 20 cm^{-1}) were also estimated. The vibrational relaxation rate ($T_1 = 1.2$ ps) has been measured independently in a pump−probe experiment.[26] The stimulated photon echo signal was calculated with the help of eqs 4.1−4.7 and 4.9 from these parameters and from the known three-dimensional structure of the peptide. Inhomogeneous broadening was modeled by summing up the third-order polarization for a set of 200 coupling Hamiltonians, where the zero-order energies were randomly chosen from uncorrelated Gaussian distribution functions with a width of 20 cm^{-1} centered at the diagonal energies (i.e., diagonal disorder). The result, which is shown in Figure 4a, is in excellent agreement with the experimental data. In particular, the first moment and the slopes on the negative and the positive

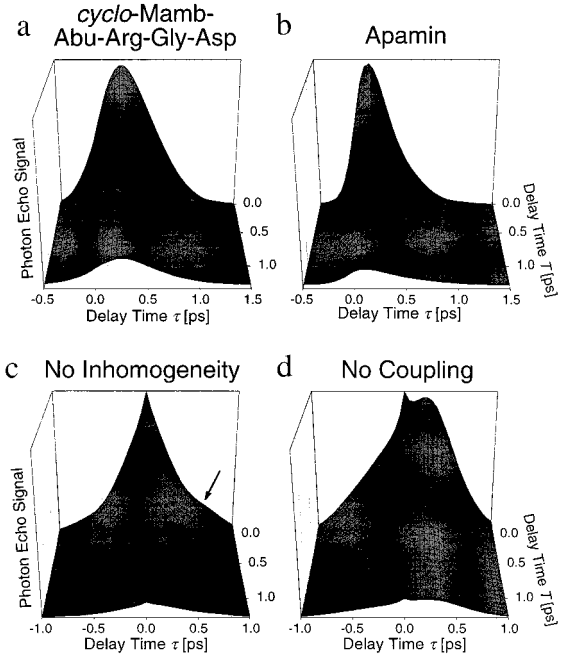

Figure 4. (a,b) Model calculation for the stimulated photon echo signal of the cyclic model peptide (*cyclo*-Mamb-Abu-Arg-Gly-Asp) and apamin, based on the known structures of these peptides, the same coupling constants as used in the model calculations to simulate the 2D-IR spectrum in refs 5 and 4, respectively, and parameters for homogeneous broadening ($T_2 = 0.7$ ps), vibrational relaxation ($T_1 = 1.2$ ps), inhomogeneous broadening (diagonal disorder 20 cm^{-1}). The pulse duration of the laser pulses was set to 120 fs. (c) The same calculation as in (a) for *cyclo*-Mamb-Abu-Arg-Gly-Asp, but with δ-shaped laser pulses and neglecting the inhomogeneous broadening. A sharp coherence spike now occurs at $T = \tau = 0$. (d) Same as in (c) but with no interaction between the states (as described by eq 4.10).

side of the τ-axis agree quite well (after a slight modification of the parameter for homogeneous broadening to 0.7 ps). A simulation of the stimulated photon echo signal on apamin is shown in Figure 4b, and again the experimental data are qualitatively reproduced. This simulation is based on the structure of apamin obtained by NMR[14] and on previously determined parameters for homogeneous broadening ($T_2 = 0.7$ ps) and diagonal disorder (24 cm^{-1}). The effect of intrapeptide hydrogen bonds on the diagonal energies was also incorporated.[4] The simulations yielded a smaller first moment for apamin than for the cyclic pentapeptide, in agreement with the experiments.

The underlying reasons for the existence of a first moment deviating so much from zero are not obvious because of the large number of terms in the computations used to fit the data, so a series of simplified model calculations were carried out. Figure 4c shows the result obtained for delta function laser pulses when inhomogeneous broadening is neglected. A sharp coherence spike is found for $\tau = T = 0$, together with a weak oscillation (see arrow). Both these effects originate from the interstate coherence terms $(1 + e^{i(\epsilon_i - \epsilon_j)T})$ which are significantly averaged out in the model calculations of Figure 4a,b by destructive interference when inhomogeneous broadening is taken into account. However, the signal is now almost a symmetric function of τ, and in contrast to the experimental data, the first moment is close to zero (note the changed range of the τ-axis). This result is unexpected, especially in view of the further simplifications of eq 4.8 that would arise if the excitonic coupling were even weaker. Then the off-diagonal anharmonicity $\Delta\epsilon_{ij}$ would be small compared with the diagonal anharmonicity $\Delta\epsilon_{ii}$ and the dephasing $1/\pi T_2$. As a consequence, in eq 4.8 the terms $(1 - e^{i\Delta\epsilon_{ij}t})e^{-t/T_2}$, for $i \neq j$, would be small compared to those for $i = j$ for any time t, so that all the terms having interstate coherence $(1 + e^{i(\epsilon_i - \epsilon_j)T})$ for $i \neq j$ would be suppressed. Equation 4.8 would then reduce to

$$\sum_{l=1}^{3} R_l = \sum_i \mu_{0,i}^4 \, e^{i\epsilon_i(\tau - t)}[1 - e^{i\Delta\epsilon_{ii}t}]e^{-(\tau+t)/T_2} \, e^{-T/T_1} \qquad (4.10)$$

which corresponds to the response of a discrete distribution of vibrational transitions.[27,28] This response is expected to give a similar result to that from a continuous distribution of frequencies over the same range:

$$\sum_{l=1}^{3} R_l = \int \mu_{0,i}^4 G(\epsilon_i) e^{i\epsilon_i(\tau - t)}[1 - e^{i\Delta\epsilon_{ii}t}]e^{-(\tau+t)/T_2} \, e^{-T/T_1} \, d\epsilon_i \qquad (4.11)$$

A model calculation according to this simplified eq 4.10 is shown in Figure 4d. Even though there is nonzero first moment, as expected, the experimentally observed slopes toward positive and negative τ's are not at all reproduced in this model calculation. Apparently eq 4.10 is not an appropriate description of the experimental situation. In other words, the distribution of zero-order energies of the amide I states (in the sense of eq 4.11) does not provide the appropriate inhomogeneity to reproduce the form of the signal. It follows that an essential contribution is made by the *inhomogeneous distribution of each individual state*, such as was used in the model calculation in Figure 4a,b.

5. Discussion and Conclusion

In contrast to the cyclic pentapeptide, the component states of the amide I band of apamin are not spectrally resolved. As a result, a complete set of diagonal elements of the coupling Hamiltonian is not available. Nevertheless, owing to the extended α-helix in this peptide, the zero-order frequencies of each individual peptide group could be very similar, so that the excitonic interaction is probably in the strong coupling limit, where the excitons are delocalized over many peptide groups. The delocalization has been estimated from the 2D-IR spectra to be on the order of 8 Å, which corresponds to ca. 4−5 peptide groups in an α-helix. Strong coupling enlarges the importance of the interstate coherence terms $(1 + e^{i(\epsilon_i - \epsilon_j)T})$, so that the first moment is made smaller. There are other important effects that need to be considered such as intramolecular interactions within the protein, intermolecular interactions with the solvent, and the influence of the different amino acid side groups on the amide I frequency, each of which could shift the amide I frequency of individual peptide groups. Therefore, a quantitative agreement between the simulated and experimentally observed peak shift is not expected for the case of apamin.

The normalized first moments M_1 from the calculated stimulated photon echo signals are shown in Figure 5. In contrast to the experimental data, they do not decay with delay time T but instead rise slightly for small T and then remain constant. The rise originates from the coherent spike at $t = 0$, which is narrower than the laser pulses and tends to lower the first moment for small T. The absence of any decay of the first moment is a consequence of the assumed Bloch description of the dynamics, which omits all spectral diffusion processes. Nevertheless, it is possible to understand the existence of a nonzero first moment within a Bloch model as shown above and this suggests a qualitative interpretation for its decay. It is well-known from MD simulations[1] as well as from photon echo experiments on spectroscopic probes embedded into pro-

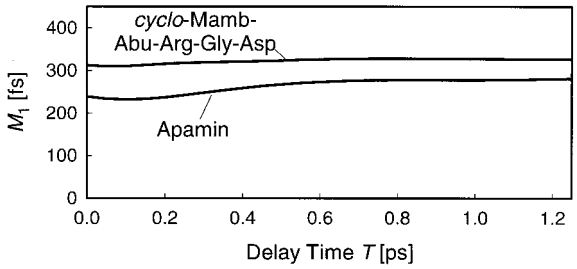

Figure 5. Normalized first moment M_1 of the calculated photon echo signals shown in Figure 4a,b. In contrast to the experimental data, no decay of the first moment is observed.

teins[6,10,12,13] that the peptide backbone is fluctuating on a wide range of time scales. The coupling scheme in the excitonic system of the amide I band must therefore be continuously rearranging on these time scales. The decay of the first moment found in the stimulated photon echo signal of both samples is considered to be a direct experimental manifestation of these fluctuations. This interpretation is consistent with the results of dynamic hole burning experiments on the amide I band, using pump pulses with a width of ca. 10 cm^{-1}. These experiments revealed a broadening of the hole width on the time scale of a few picoseconds.[4] Mukamel and co-workers have developed a description of spectral diffusion processes in excitonic systems[23,24] which goes beyond the Bloch picture. Such a theory should be adequate to model the *T*-dependence of the stimulated photon echo signal, and in association with MD simulations, should enable the amplitudes and time scales of these peptide fluctuations to be assessed by experiments.

The observation window for spectral diffusion processes is limited to ca. 1.2 ps by the rapid vibrational relaxation of the amide I state. Nevertheless, MD simulations indicate that a significant fraction of the correlation function of the peptide fluctuations indeed decays on this time scale (see, for example, ref 2). The transient grating signal, measured at $\tau = 0$, exhibits a biphasic decay with time constants 250 and 600 fs (Figure 2). The latter time constant perfectly matches half the vibrational relaxation time $T_1 = 1.2$ ps of the amide oscillator,[4] as expected in an experiment that measures the square of the response (i.e., a homodyne detection scheme). The faster time constant originates from the coherence (Figure 4c) and is due to dephasing of the interstate coherence terms in eq 4.8.

The peptides do not have any symmetry associated with the interchange of the amide units so transitions between all possible states can contribute to the echo and transient grating signals. Nevertheless, the photon echo first moment decays are signaling the *T*-dependent inhomogeneity of the set of excitonically coupled, inhomogeneously broadened states. The results are conceptually similar to those found for optical transitions of the photosynthetic antennae[10,29] and J-aggregates[30] modeled as coupled two-level systems. However, our results provide a measure of spectral diffusion processes determined by all the peptide groups and the interactions between them. At this point it is not possible to establish the dominating mechanism. The spectral diffusion could be either population equilibration between excitonic states or diffusion of the diagonal energies, such as might occur during the formation and breaking of hydrogen bonds, perhaps involving solvent. Other nonlinear experimental schemes, such as frequency-resolved or heterodyne-detected three-pulse photon echo experiments, would reveal three-dimensional data sets and thus might provide the additional spectroscopic information needed to reconstruct the complete response functions.

Acknowledgment. We thank Dr. Nien-Hui Ge for helpful discussions. The research was supported by the NSF and NIH and used instrumentation developed from NIH Grant RR01348. P.H. thanks the Deutsche Forschungsgemeinschaft for a post-doctoral fellowship.

References and Notes

(1) Karplus, M.; Petsko, G. A. *Nature* **1990**, *347*, 631.
(2) Zhou, H. X.; Wlodek, S.; McCommon, *J. A. Proc. Natl. Acad. Sci. U.S.A.* **1998**, *95*, 9280.
(3) Elber, R.; Karplus, M. *J. Am. Chem. Soc.* **1990**, *112*, 9161.
(4) Hamm, P.; Lim, M.; Hochstrasser, R. M. *J. Phys. Chem. B* **1998**, *102*, 6123.
(5) Hamm, P.; Lim, M.; DeGrado, W. F.; Hochstrasser, R. M. *Proc. Natl. Acad. Sci. U.S.A.* **1999**, *96*, 2036.
(6) Lim, M.; Hamm, P.; Hochstrasser, R. M. *Proc. Natl. Acad. Sci. U.S.A.* **1998**, *95*, 15315.
(7) Krimm, S.; Bandekar, J. *Adv. Protein Chem.* **1986**, *38*, 181.
(8) Torii, H.; Tasumi, M. *J. Chem. Phys.* **1992**, *96*, 3379.
(9) Ernst, R. R.; Bodenhausen, G.; Wokaun, A. *Principles of Nuclear Magnetic Resonance in One and Two Dimensions*; Oxford University Press: Oxford, UK, 1987.
(10) Joo, T.; Jia, Y.; Yu, J. Y.; Jonas, D. M.; Fleming, G. R. *J. Phys. Chem.* **1996**, *100*, 2399.
(11) d. Boeij, W. P.; Pshenichnikov, M. S.; Wiersma, D. A. *Chem. Phys. Lett.* **1996**, *253*, 53.
(12) Groot, M.-L.; Yuj., Y.; Agarwal, R.; Norris, J. R.; Fleming, G. R. *J. Phys. Chem. B* **1998**, *102*, 5923.
(13) Leeson, D. T.; Wiersma, D. A.; Fritsch, K.; Friedrich, J. *J. Phys. Chem. B* **1997**, *101*, 6331.
(14) Pease, J. H. B.; D. Wemmer, D. E. *Biochemistry* **1988**, *27*, 8491.
(15) Bach, A. C.; Eyermann, C. J.; Gross, J. D.; Bower, M. J.; Harlow, R. L.; Weber, P. C.; DeGrado, W. F. *J. Am. Chem. Soc.* **1994**, *116*, 3207.
(16) Hamm, P.; Lim, M.; Hochstrasser, R. M. *J. Chem. Phys.* **1997**, *107*, 10523.
(17) Levenson, M. D.; Kano, S. S. *Introduction to Nonlinear Laser Spectroscopy*; Academic Press: Boston, 1988.
(18) Hamm, P.; Lim, M.; Hochstrasser, R. M. *Phys. Rev. Lett.* **1998**, *81*, 5326.
(19) Silvestri, S. D.; Weiner, A. M.; Fujimoto, J. G.; Ippen, E. P. *Chem. Phys. Lett.* **1984**, *112*, 195.
(20) Joo, T.; Albrecht, A. C. *Chem. Phys.* **1993**, *176*, 233.
(21) Joo, T.; Jia, Y.; Yu, J.-Y.; Lang, M.-J.; Fleming, G. F. *J. Chem. Phys.* **1996**, *104*, 6089.
(22) Cho, M.; Yu, J.-Y.; Joo, T.; Nagasawa, Y.; Passino, S. A.; Fleming, G. R. *J. Phys. Chem.* **1996**, *100*, 11944.
(23) Meier, T.; Chernyak, V.; Mukamel, S. *J. Chem. Phys.* **1997**, *107*, 8759.
(24) Chernyak, V.; Zhang, W. M.; Mukamel, S. *J. Chem. Phys.* **1998**, *109*, 9587.
(25) Mukamel, S. *Principles of Nonlinear Optical Spectroscopy*; Oxford University: New York, 1995.
(26) Hamm, P.; Lim, M.; Hochstrasser, R. M., to be published.
(27) Rector, K. D.; Kwok, A. S.; Ferrante, C.; Tokmakoff, A.; Rella, C. W.; Fayer, M. D. *J. Chem. Phys.* **1997**, *106*, 10027.
(28) Hamm, P.; Lim, M.; Asplund, M.; Hochstrasser, R. M. *Chem. Phys. Lett.* **1999**, *301*, 167.
(29) Jimenez, R.; Mourik, F.; Yu, J. Y.; Fleming, G. R. *J. Phys. Chem. B* **1997**, *101*, 7350.
(30) Fidder, H.; Wiersma, D. A. *J. Phys. Chem.* **1993**, *97*, 11603.